Materials Science-Poland, 41(1), 2023, pp. 140-160
http://www.materialsscience.pwr.wroc.pl/
DOI: 10.2478/msp-2023-0010

Influence of elevated temperature on the engineering properties of ultra-high-performance fiber-reinforced concrete

Aref A. Abadel[1,*], M. Iqbal Khan[1], Radhouane Masmoudi[2]

[1]Department of Civil Engineering, College of Engineering, King Saud University, Riyadh 1142, Saudi Arabia
[2]Department of Civil and Building Engineering, University of Sherbrooke, Sherbrooke, Canada

This paper investigates the effect of high temperatures on the compressive strength, flexural strength, and splitting tensile strength of ultra-high-performance concrete (UHPC), and ultra-high-performance, fiber-reinforced concrete (UHPFRC). The experimental variables in this study were fiber type, fiber content, and high-temperature exposure levels. Three different types of fibers were evaluated, including steel fibers, polypropylene (PP), and polyvinyl alcohol (PVA) fibers. Six concrete mixes were prepared with and without different combinations of fibers. One mix was made with no fibers. Others were made with either steel fibers alone; a hybrid of steel fibers and PVA; and a hybrid system of steel, PP, and PVA fibers. These mixes were tested under a range of temperatures and compared for strength. The UHPC and UHPFRC were exposed to high temperatures at 100°C, 300°C, 400°C, and 500°C for 3 hours. The results showed that UHPFRC did not exhibit any significant degradation when exposed to 100°C. However, reductions of approximately 18% to 25%, 12% to 22%, and 14% to 25% in the compressive strength, splitting tensile strength, and flexural strength were observed when the UHPFRC was exposed to 400°C. UHPFRC made of steel fibers showed higher mechanical properties after exposure to 400°C compared to UHPFRC made of PP and PVA fibers. The results also demonstrate the use of PVA and/or PP fibers, along with steel fiber, to withstand the effects of highly elevated temperature and prevent spalling of UHPC after exposure to elevated temperature. The observed spalling was a direct result of the melting and evaporation of PVA and/or PP fibers when exposed to high temperature, an effect that was confirmed using scanning electron microscopy.

Keywords: *UHPC, UHPFRC, fibers, concrete, mechanical properties, high temperature*

1. Introduction

In the current state of construction and building materials, ultra-high-performance concrete (UHPC) has gotten a great deal of attention because of its excellent compressive strength of higher than 120 MPa and various strength, physical, and durability properties [1, 2]. UHPC's uniformity and packed microstructure provide high-strength characteristics [3], which are improved by removing the coarse crushed stone aggregates and employing finer sized materials such as silica fume, quartz sand, and ordinary Portland cement (OPC), etc., [4] and a very low water-to-cement ratio (w/c), which minimizes internal flaws of UHPC such as microcracks and voids [5–7]. The ductility of UHPC is improved by introducing steel, polypropylene, or polyvinyl alcohol fibers [8–10]. The addition of nanomaterials has been noted to strengthen the dynamic, strength, and static properties of UHPC [11, 12]. Adding to its superior strength characteristics, ultra-high-performance concrete also has outstanding endurance against the infiltration of harmful elements, which minimizes the danger of steel corrosion [13, 14]. Even though the amount of OPC is very high, it has good endurance against shrinking because of its low water-to-binder percentage [15]. The excellent shrinkage resistance of UHPC is because of the UHPC's higher tensile strength, offered by packed microstructure and steel or polypropylene fibers [16, 17]. Furthermore, UHPC also has good resistance against abrasion, which is particularly significant in industrial floorings and bridge decks [18, 19].

Concrete typically has good resistance to highly

* E-mail: aabadel@ksu.edu.sa

elevated temperature exposure in comparison to other building materials such as steel [20–22]. Concrete can suffer degradation, however, when subjected to highly elevated temperatures due to thermal spalling [23–26]. Thermal spalling is caused mainly by three mechanisms: The first mechanism is the decomposition of the cement matrix, causing a reduction in the compressive strength [27]. The second mechanism is the development of significant stresses between the surface and the core of the concrete due to the formation of a thermal gradient. The third mechanism is the increase in the vapor pressure caused by the evaporation of free and chemically bonded water and the decomposition of other hydrated phases in the paste portion of the concrete. These three mechanisms depend mainly on concrete tensile strength, thermal conductivity, thermal expansion coefficient, permeability and thermal diffusivity [28–30]. Recently, Mróz and Hager [31] developed a new method for assessing the form and intensity of the nature of different types of spalling (surface spalling, explosive spalling, aggregate spalling) through signal amplitude analysis. Abadel et al. [32] studied the residual compressive strength and spalling of normal and high-strength concrete with and without fiber after exposure to various heating and cooling regimes. Their findings showed that hybrid fiber can prevent the spalling of concrete structures. Zhang et al. [33] found that the addition of natural fibers to UHPC can also improve its thermal spalling resistance.

Reports in the literature have evaluated the impact of temperatures exposure on compressive strength, and elastic modulus of concrete structures fairly well. However, the outcome shows a variation in the results. Some studies showed no significant impact on the concrete compressive strength and elastic modulus when exposed to elevated temperatures of up to 400°C, while others showed significant losses. On the other hand, research studies showed that porosity and permeability of the concrete increased with exposure to high temperatures [34, 35]. This can be attributed to the development of microcracks caused by the vapor pressure, thermal expansion, and decomposition of hydration products.

UHPC and ultra-high-performance fiber reinforced concrete (UHPFRC) have much lower porosity and permeability than traditional concrete, increasing the risk of thermal spalling and damage [36–38]. This is due to the smaller available space in UHPC and UHPFRC that can accommodate the released vapors due to the lower porosity and the slower release of the internal vapor pressure due to the low concrete permeability. This causes the degradation of UHPC and UHPFRC to occur at lower temperatures compared to traditional concrete. Research studies have shown that the degradation of UHPC and UHPFRC can be initiated at high temperatures between 200°C and 300°C. Other studies have shown that strength loss in UHPC and UHPFRC under stress can start at temperatures as low as 100°C. However, this loss is insignificant compared to the loss that can occur when exposed to high temperatures greater than 500°C [39, 40]. Spalling caused by high temperatures can reduce the cross-sectional area of the concrete element and expose the reinforced steel rebars, causing further implications.

The type of fibers used in UHPFRC can impact fire resistance. Research studies have shown that steel and polypropylene (PP) fibers can reduce the risk of thermal spalling and damage [41–43]. The polyvinyl alcohol (PVA) and PP fibers melt and evaporate when the concrete is exposed to high temperatures, creating pressure relief passages for the internal vapor pressure. Studies have shown that the use of 0.6% PP fibers effectively improves the fire resistance of UHPFRC [44]. A combination of fibers such as steel and synthetic PP fibers can provide an optimal solution due to the increased ductility and thermal resistance [18, 19, 24]. Although research work on the effect of high temperature on UHPC made with PP fibers has been conducted, more research in this area is required [46].

Given the critical applications for which UHPC and UHPFRC are used, as well as the fact that these are relatively modern products, it is quite important to comprehend the impact of high temperatures on the mechanical characterization and durability of UHPC and UHPFRC. In addition, further research is required due to the existence of contradictory findings observed in the literature regarding the im-

Table 1. Cement and silica fume properties

		Type 1 Cement	Silica Fume
Chemical composition (%)	CaO	64.1	2.15
	SiO_2	21.8	89.5
	AL_2O_3	5.25	0.43
	Fe_2O_3	4.10	3.25
	MgO	0.71	1.30
	TiO_2	0.3	0.0
	SO_3	2.4	0.74
Physical properties	L.O.I	2.18	2.47
	Mean particle size (μm)	40.1	0.32
	Specific gravity	3.15	2.2

Table 2. UHPC mixture proportions for 1 m^3

Material	Weight (kg/m^3)
Cement	900.0
Fine quartz sand	1000.0
Silica Fume	222.0
Water	164.0
Super-plasticizer	30

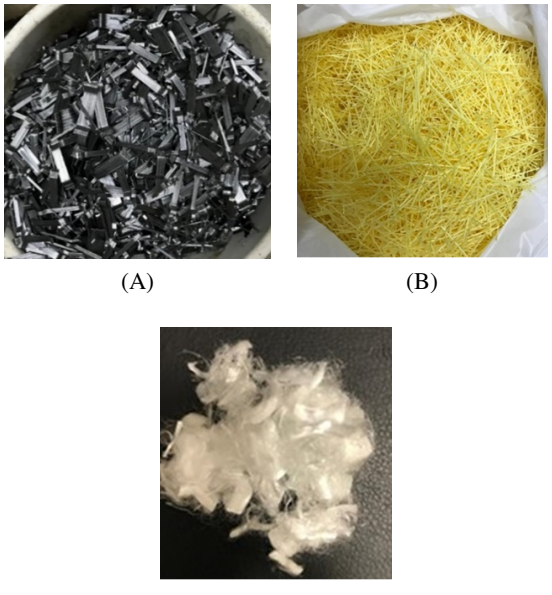

(A) (B)

(C)

Fig. 1. Fibers: (A) hooked-steel fibers; (B) polyvinyl alcohol fibers (C) polypropylene fibers

pact of highly elevated temperature on UHPC and UHPFRC. A limited number of studies have investigated the behavior of UHPC with different types (hybrid) of fiber after temperature exposure. This paper aims to evaluate the impact of high temperature on the mechanical properties of UHPC and UHPFRC. Furthermore, the effect of using different types of fibers on the behavior of UHPC when exposed to high temperatures is also evaluated.

2. Experimental program

2.1. Material properties and mixture

The chemical composition based on X-ray fluorescence (XRF) analysis and physical properties of Portland ASTM International Type-I cement and silica fume used in this study are shown in Table 1. The sand used was dense quart sand with a maximum particle size of 2 mm. The mixture proportions are presented in Table 2. All concrete mix designs had a cement content of 900 kg/m^3 and 222 kg/m^3 of micro silica. The sand content was 1000 kg/m^3 in all mixes. All mixes had a w/b (cement and silica fume) ratio of 0.146. The workability of concrete was maintained using a superplasticizer at a dosage of 30 kg/m^3. This work evaluated three types of fiber: steel, PVA, and PP fibers, as shown in Figure 1. Table 3 summarizes the properties of all fibers. The steel fibers used were hook-ended with a length of 30 mm and 0.5 mm in diameter. The tensile strength of the steel fibers was 1225 MPa, and the modulus of elasticity was 200 GPa. The PVA fibers were 30-mm straight fibers with a tensile strength of 900 MPa, and elasticity modulus of 23 GPa. The PP fibers were 12-mm straight

Table 3. Properties of fibers

Fiber type	Fiber properties					
	Shape	Length (mm)	Section dimension (mm)	Specific gravity	Modulus of elasticity (GPa)	Tensile strength (MPa)
Steel fibers	Hooked ends	35	φ 0.55 (Circular)	7.85	210	1225
Polyvinyl alcohol (PVA)	straight	30	φ 0.66 (Circular)	1.3	23	900
Polypropylene (PP)	straight	12	φ 0.022 (Circular)	0.90	4	550

Table 4. Percentage of fibers in concrete mixes

Concrete mix	Fiber by volume (%)		
	Polyvinyl alcohol (PVA)	Polypropylene (PP)	Steel fibers (SF)
M0-NF	0.0	0.0	0.0
M1-S1	0.0	0.0	1.0
M2-S0.7-PVA0.3	0.3	0.0	0.7
M3-S0.7-PVA0.2-PP0.1	0.2	0.1	0.7
M4-S0.7-PVA0.2	0.2	0.0	0.7
M5-S0.5-PVA0.5	0.5	0.0	0.5

Table 5. Details of test matrix

Mix	Compression and split Test				Flexure Test			
	Room temp.	100°C	300°C	400°C	Room temp.	100°C	300°C	400°C
M0-NF	6	6	6	6	3	3	3	3
M1-S1	6	6	6	6	3	3	3	3
M2-S0.7-PVA0.3	6	6	6	6	3	3	3	3
M3-S0.7-PVA0.2-PP0.1	6	6	6	6	3	3	3	3
M4-S0.7-PVA0.2	6	6	6	6	3	3	3	3
M5-S0.5-PVA0.5	6	6	6	6	3	3	3	3

fibers with a tensile strength of 550 MPa and modulus of elasticity of 4 GPa. Table 4 shows the percentage by volume of fibers used in each mix design.

2.2. Test matrix and specimen preparation

Different concrete mixtures were evaluated in this study, as shown in Table 4. To examine the impact of incorporating various types of fibers, the hybrid UHPC mixes were classified into five groups. It was ensured that the overall volume fraction of fibers remained constant at 1% by volume across all mixes. Out of six mix designs, the first mix was a UHPC control mix with no fibers (M0-NF), and the remaining five mixes included fibers (i.e., UHPFRC). The second mix (M1-S1) is UHPFRC made with 1% by volume of steel fibers. The third mix (M2-S0.7-PVA0.3) is UHPFRC made with a hybrid fiber system of 0.7% by volume of steel fibers and 0.3% by volume of PVA fibers. The fourth mix (M3-S0.7-PVA0.2-PP0.1) was made of a hybrid system consisting of 0.7% by volume of steel fibers, 0.2% by volume of PVA fibers and 0.1% by volume of PP fibers. A hybrid fiber made of 0.7% by volume of steel fibers and 0.2% by volume of PVA fibers was used in the fifth mix and 0.5% by volume of steel fibers and 0.5% by volume of PVA fibers were used in the sixth mix. For

each of the six mixes, twenty-four 100 mm × 200 mm cylinders and eight 150 mm × 150 mm × 600 mm prisms were cast, as shown in Table 5. The cylinders were used for compressive and split tensile strength testing, while the concrete prisms were used for flexural testing. For each mix design, six cylinders and three prisms were tested for each exposure temperature considered in this study (i.e., room temperature at 26°C, 100°C, 300°C, 400°C, and 500°C).

For all concrete cylinder samples, plastic molds were used, and the concrete was filled in a single layer. Concrete prisms were created by pouring concrete into steel molds. The concrete surface was finished with a steel trowel after casting. After 24 hours of humid curing at ambient temperature, the concrete prisms and cylinders were removed from the molds and then cured in water for 28 days.

2.3. Heating of specimens

At the end of the 28-day water curing, the specimens of concrete were air dried at ambient temperature for 28 days to ensure the concrete was dry before exposure to highly elevated temperatures. This was to allow the drying shrinkage to occur before the sudden increase in temperature. An electric oven with clear dimensions of 1000 mm × 1000 mm × 1000 mm was used. The concrete samples were exposed to the heated regime at a rate of 8°C/min. Heating curves for each heating regime (i.e., 100°C, 300°C, 400°C, and 500°C) are shown in Figure 2. This figure also includes the curve of heating as per ISO 834 [47]. The temperature of the oven was controlled using a Type-K thermocouple. Once the oven temperature reached the maximum temperature (i.e., 100°C, 300°C, 400°C, and 500°C), the temperature was sustained for three hours. After being heated, all types of concrete samples were cooled down to ambient temperature before testing.

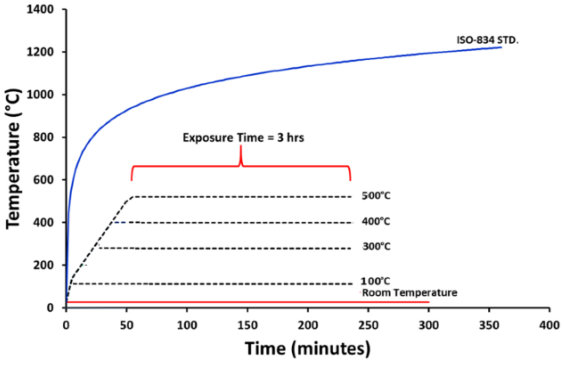

Fig. 2. Individual time-temperature plots

2.4. Testing procedures

The fresh concrete properties were measured using slump flow according to ASTM C143 [48], and the concrete unit weight was evaluated according to ASTM C138 [49]. The concrete hardened properties were evaluated using compressive and splitting tensile strength as well as flexural strength. The concrete compressive strength was

Fig. 3. Specimen under testing

(A) Before testing

(B) After testing

Fig. 4. Prism specimen in flexure test

evaluated as per ASTM C39 [50]. Before testing, the concrete cylindrical samples were capped with sulfur capping to ensure a leveled testing surface. During the compressive strength testing, axial strain was measured using a compressometer made of two linear variable differential transformers (LVDTs), as shown in Figure 3. The elastic modulus was evaluated as per ASTM C469 [51]. The splitting tensile strength was evaluated in accordance with ASTM C496 [52]. The flexure strength was measured using a three-point bending test based on ASTM C78 [53]. The flexural testing was deflection controlled with a 0.25 mm/min displacement rate until failure. The mid-span deflection was measured using (LVDTs), as shown in Figure 4. The load and deflection were recorded using a data acquisition system. The mass loss of the samples was determined based on the weight of specimens before and after exposure to elevated temperature using a precise weighing scale. Furthermore, microstructural analysis was also performed through SEM micrographs to evaluate the microstructure of the UHPGC specimens using the instrument (JOEL JSM-7600F Scanning Electron Microscope) available at King Saud University.

3. Experimental results and discussion

3.1. Fresh concrete properties

The fresh concrete properties, including the slump flow and unit weight, are presented in Table 6. All mixes showed good workability with no bleeding or fiber segregation. The slump flow of the control mix without fibers (i.e., M0-NF) was 280 mm, which was greater than the slump of the UHPFRC mixes that ranged from 250 mm to 257 mm. The lower slump in the UHPFRC mixes is due to the existence of fibers. The unit weight of all mixes ranged from 2285 kg/m^3 to 2363 kg/m^3.

Table 6. Fresh UHPC properties

Mix No.	Unit Weight (kg/m^3)	Slump (mm)
M0-NF	2318	280.0
M1-S1	2363	257.0
M2-S0.7-PVA0.3	2325	256.0
M3-S0.7-PVA0.2-PP0.1	2294	250.0
M4-S0.7-PVA0.2	2310	255.0
M5-S0.5-PVA0.5	2285	251.0

3.2. Effect of temperature exposure

Figures 5 and 6 present the concrete specimens after exposure to high temperatures. Concrete samples heated to 300°C, 400°C, and 500°C showed discoloration, whereas no discoloration was observed in specimens heated to 100°C. For concrete samples heated to 100°C, no spalling or cracking was observed. Concrete specimens made without fibers (i.e., M0-NF) and heated to 300°C showed thermal cracking at the surface, which aligns with the findings of other research in the literature [54, 55]. On the other hand, UHPFRC specimens showed no thermal cracking due to fibers that contributed to the bridging effect of cracks. At 400°C, concrete specimens made without steel fibers (i.e., M0-NF) and concrete specimens made with steel fibers alone (i.e., M1-S1) showed spalling at the end and the corner surfaces of the specimens. This spalling can be due to the dense microstructure of the concrete, which makes it difficult for the water vapor to escape, causing significant internal pressure at these locations. Previous research has indicated that concrete spalling can be attributed to the accumulation of internal pressure, thermal stresses, and thermal cracking [56]. The absence of PP and PVA fibers could also contribute as these synthetic fibers melt and evaporate at about 270°C and 170°C, respectively, leaving venting tunnels to minimize the existing internal vapor pressure [4]. The concrete samples made with PP and PVA fibers showed significantly lower spalling and cracking compared to concrete specimens made without PVA and PP fibers. At 500°C, all concrete specimens showed significant spalling, as demonstrated in Figure 6. Therefore, no testing could be conducted on concrete after exposure to 500°C. It was observed from the protruding steel fibers from the failing specimens that the steel fibers were well distributed.

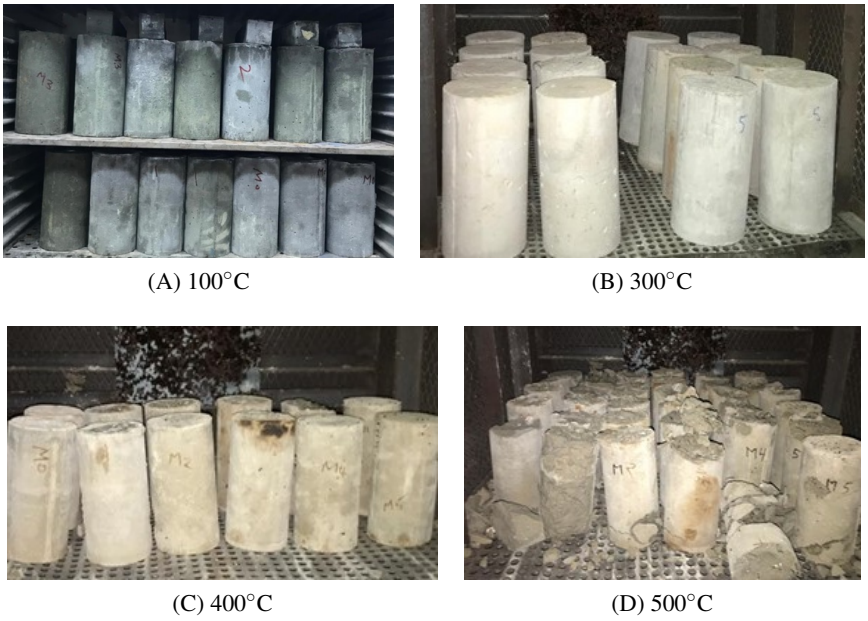

(A) 100°C (B) 300°C

(C) 400°C (D) 500°C

Fig. 5. All samples after heating-cooling cycle

Fig. 6. Destroyed concrete specimen from 500°C exposure

3.3. Compressive strength

The results of the residual compressive strength are given in Table 7. Figure 7 presents the concrete specimens after the compressive strength testing. Every single value in this table shows the average of three consecutive samples. This table also shows the percentage loss of compressive strength to the initial compressive strength before exposure to high temperatures. As mentioned previously, concrete samples exposed to high temperature at 500°C could not be tested due to the significant degradation during heating. Concrete specimens exposed to high temperatures had minimal residual compressive strength compared with samples that had not been subjected to high temperatures. It was noted that the residual compressive strength of the concrete mixes dropped as the temperature rose, regardless of fiber content or type.

For concrete samples exposed to ambient temperature, steel fibers increased the compressive strength by 16% in comparison with bare mix (i.e., mix M0-NF). As demonstrated in Table 6, concrete samples produced with a hybrid matrix comprising steel, PP, and PVA fibers increased their compressive strength by about 10%. In comparison to the control mix, the compressive strength improved by 7% to 12% when a combination of PVA and steel fibers was utilized (i.e., mix M0-NF).

For concrete samples exposed to high temperatures between 100°C and 400°C, the use of a combination of fiber systems effectively increased the

Table 7. Summary of test results of different concrete mixes

Mix	Compressive strength (MPa)				Flexure strength (MPa)				Splitting strength (MPa)			
	Room temp.	**100°C**	**300°C**	**400°C**	**Room temp.**	**100°C**	**300°C**	**400°C**	**Room temp.**	**100°C**	**300°C**	**400°C**
M0-NF	120.3	124.1 (+3%)	105.6 (−12.5%)	88.32 (−26.6%)	10.27	10.47	8.77 (−15.1%)	7.50 (−27.0%)	6.6	6.8 (+3%)	5.7 (−13.6%)	4.80 (−27.3%)
M1-S1	139.8 (16.2%)	143.8 (+2.9%)	132.0 (−5.5%)	104.68 (−25.12%)	19.50 (89.9%)	19.75	17.83 (−9.0%)	16.20 (−17.0%)	11.7 (77.3%)	11.9 (+3%)	10.8 (−7.7%)	10.20 (−12.8%)
M2-S0.7-PVA0.3	134.6 (11.8%)	139.4 (+3.6%)	123.4 (−8.5%)	110.19 (−18.2%)	19.00 (85%)	19.53	17.24 (−9.0%)	15.10 (−20.5%)	12.3 (86.4%)	12.7 (+3%)	11.9 (−3.3%)	10.70 (−13%)
M3-S0.7-PVA0.2-PP0.1	131.7 (9.5%)	133.7 (+1%)	129.7 (−1.0%)	102.62 (−21.5%)	17.03 (65.8%)	17.64	16.00 (−6.0%)	15.20 (−10.7%)	12.1 (83.3%)	12.4 (+3%)	11.4 (−5.8%)	10.40 (−14%)
M4-S0.7-PVA0.2	128.2 (6.8%)	130.3 (+1%)	124.0 (−3.3%)	99.70 (−22.3%)	17.77 (73%)	17.85	17.01 (−4.0%)	14.20 (−20.0%)	11.7 (77.3%)	11.8 (+3%)	10.9 (−6.8%)	9.50 (−18.8%)
M5-S0.5-PVA0.5	127.8 (6.5%)	131.8 (+3.2%)	119.6 (−6.4%)	97.4 (−23.7%)	16.90 (64.5%)	17.0	15.85 (−6.0%)	12.90 (−25.0%)	11.3 (74.2%)	11.8 (+3%)	10.8 (−6.1%)	8.90 (−22.6%)

* The percentage decrease with respect to the ambient temperature is represented by the value enclosed in parentheses.
** The percentage increase in the samples made without fiber is represented by the value within in parentheses.

(A)

(B)

(C)

Fig. 7. Representative samples after compression testing: (A) 100°C; (B) 300°C (C) 400°C

residual compressive strength after being subjected to high temperatures with respect to concrete samples containing no fibers. This is due to fibers' capacity to regulate thermal cracking and internal vapor pressure venting caused by the melting and evaporation of PVA and PP fibers at high temperatures [57, 58].

It was observed that concrete specimens exposed to 100°C temperatures showed a 1% to 4% increase in compressive capacity, which was identical to the same concrete specimens exposed to ambient temperature. This can be attributed to the additional hydration reactions as a result of heating to 100°C. The exposure to 100°C increases the ionic movement of ions and water vapor, which causes a portion of the unhydrated cement particles to react, causing increased hydration products and thus increased strength. In a study by Hager et al. [59], similar observations were reported; they stated that the reduction in strength may be caused by the cracking of the cement paste around quartz aggregates, which expand at higher temperature such as 400–500°C due to the transformation from β quartz to α quartz. Similar findings and explanations were observed in earlier studies [59], where this occurrence was attributed to the phenomenon of internal autoclaving. Moisture is transformed into water vapor as a result of heating. Under these conditions, chemical and physical changes may take place. The process of simultaneously exposing the material to high pressure and temperature is a well-known technology in the prefabrication of concrete. This procedure may activate changes in the microstructure of hydrates and often increases concrete strength. Another study by Peng at al. [60] showed that the degree of C-S-H decomposition depends on the heating temperature and duration. At higher temperatures, the C-S-H gel decomposed into crystalline phases such as calcium oxide (CaO) and silica (SiO_2), leading to a loss of strength in the material. As the temperature continued to in-

crease, these crystalline phases underwent further reactions leading to the formation of calcium aluminosilicate and wollastonite. After exposure to high temperature at 300°C, however, the control mix (i.e., M0-NF) without fibers showed approximately 13% reduction in strength under compression, which was the greatest reduction observed compared to other concrete mixes made with fibers. Concrete specimens exposed to high temperature at 300°C showed a decrease of approximately 6% when steel fibers were used (i.e., M1-S1) compared to the same mix exposed to room temperature. Concrete samples made with a combination of steel and synthetic PVA fibers reveal a reduction in the compressive strength ranging from 3% to 9%. Compared to the same mix exposed to room temperature, no significant reduction in the compressive strength was found in concrete samples prepared using a combination of steel, PVA, and PP fibers when exposed to 300°C compared to the same mix exposed to room temperature.

At 400°C, the control mix without fibers showed an approximately 27% reduction in compressive strength. A similar reduction in the compressive strength was reported in concrete samples containing steel fibers only. The residual compressive strength was enhanced by using a hybrid fiber system instead of steel fibers. The compressive strength of concrete samples made with a combination of PVA, and steel fibers was reduced by 18% to 24%. The compressive strength of concrete samples composed of hybrid fibers (i.e., steel, PVA, and PP) was reduced by about 22%.

The compressive strength of all mixes showed that the exposure to high temperature at 400°C caused significant strength loss compared to exposure to a temperature of 300°C. Compared to concrete with no fibers, the use of fibers caused a significant increase in the residual compressive strength after exposure to 300°C compared to concrete without fibers. However, at 400°C the use of fibers was less effective in increasing the residual strength compared to what was observed at 300°C. In general, using a combination of steel, PVA, and PP fibers was more effective in increasing the concrete residual compressive strength after exposure to high temperatures at 300°C and 400°C. Scheinherrová et al. [61] performed another study and found that reactive powder concrete with 2% Cu-Zn-coated steel fibers had the highest residual compressive strength after being exposed to high temperatures up to 800°C. This was compared to samples without fibers and samples with uncoated steel fibers. The Cu-Zn layer on the steel fibers prevented the fibers from rusting and made it easier for the fibers to stick to the matrix. This made the material better at resisting loss of compressive strength at high temperatures.

3.3.1. Stress-strain relationships

It's crucial to assess the stress-strain response of concrete, especially when it's subjected to high temperatures. The stress-strain plots of concrete samples exposed to 26°C, 300°C, and 400°C, respectively, are shown in Figures 8, 9, and 10. From the above-mentioned figures, it can be noted that concrete specimens exposed to ambient temperature showed greater elastic modulus compared to similar concrete mixes exposed to high temperatures at 300°C and 400°C. Concrete mixtures exposed to 400°C showed the lowest modulus of elasticity. On the other hand, concrete mixes exposed to 300°C and 400°C showed higher ductility and energy dissipation compared to similar concrete mixes exposed to room temperature. Furthermore, it was observed that for UHPFRC samples exposed to high temperature at 400°C, the stiffness reduction was more pronounced than the reduction in the compressive strength. This could be attributed to the degradation of the concrete matrix and the development of thermal cracks [62]. UHPFRC made with steel fibers showed considerable energy absorption and better elastic modulus (i.e., area under the plots of stress-strain) compared to concrete samples made with no fibers or UHPFRC made with a hybrid system. This is expected, because steel fibers exhibit greater modulus of elasticity and tensile strength compared to PVA and PP fibers. In addition, steel fibers have better high-temperature resistance compared to PVA and PP fibers. On the basis of previous studies [63, 64], UHPC and UHPFRC have different stress-strain behaviors due to the presence of different types of reinforcements. UHPC has a high elastic modulus

and exhibits strain-softening behavior after peak stress, while UHPFRC has a similar elastic modulus, but shows a plateau or gradual reduction in stress after peak stress due to the fiber bridging effect. The addition of fibers to UHPFRC also results in improved ductility and crack resistance, making it more suitable for structural applications that require high-performance concrete.

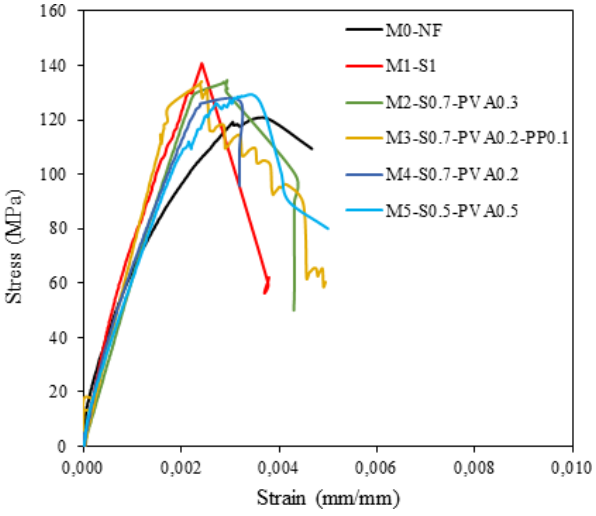

Fig. 8. Stress-strain relations for UHPFRC cylinders at ambient temperature

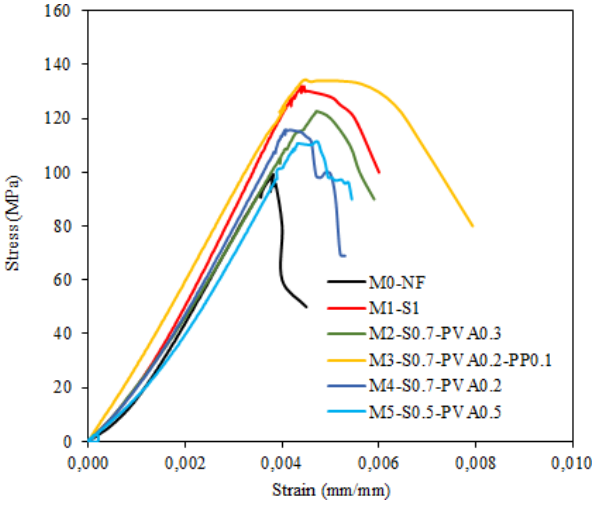

Fig. 9. Stress-strain relations for UHPFRC cylinders at 300°C

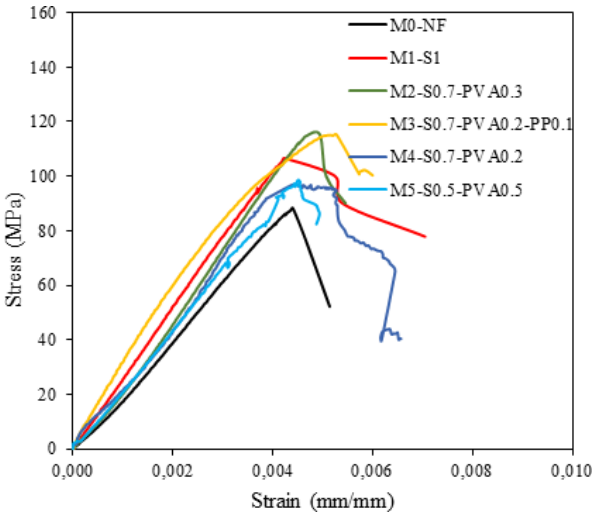

Fig. 10. Stress-strain relations for UHPFRC cylinders at 400°C

3.3.2. Mode of failure

The failure modes of the concrete compressive strength samples exposed to high temperatures of 100°C, 300°C, and 400°C are shown in Figure 7. Concrete specimens made without or with fibers and subjected to ambient temperature failed in a sudden and explosive manner compared to similar mixes exposed to temperatures of 300°C and 400°C. It is noted that the mode of failure was quite ductile in concrete samples with fibers subjected to 300°C and 400°C compared to that in concrete specimens without fibers. Compared to all other concrete mixes, specimens made with a hybrid PVA and PP fiber system demonstrated the greatest ductile behavior. This can be because the melting and evaporation of these fibers at severe temperatures will generate venting channels that minimize the inner vapor pressure. Several studies have investigated the failure modes of UHPC when exposed to high temperatures. One common failure mode observed in UHPC without fibers is sudden and explosive failure, known as spalling, which occurs as the result of the buildup of internal pressure resulting from the release of water vapor from the hydrated cement paste at high temperatures [65, 66]. Spalling can cause significant damage to concrete structures and compromise their structural integrity. The addition of fibers to UHPC

can help to mitigate spalling and improve the ductility of the material under high temperatures. The fibers act as crack arresters and help to distribute the stresses more evenly, resulting in a more ductile failure mode [67]. In addition, the fibers can help to increase the porosity of the concrete when they melt or evaporate, which can further reduce the risk of spalling and improve the material's ductility [68]. The failure modes observed in UHPC with hybrid fibers when exposed to high temperatures appear to be more ductile compared to those of UHPC without fibers or with only steel fibers. The study by Thahwia et al. [68] found that UHPC with a hybrid PVA and PP fiber system demonstrated the greatest ductility, likely due to the melting and evaporation of the fibers, which increased the porosity of the concrete. This finding is consistent with the results reported by Gong et al. [69], who found that the addition of hybrid fibers to UHPC improved its ductility and energy absorption capacity.

3.4. Flexural strength

Figures 11 through 13 present the load versus mid-span deflection curves for concrete specimens exposed to ambient temperature, 300°C, and 400°C. Figure 14 shows the failure modes of the flexural specimens. All concrete mixes showed a linear load-displacement response before reaching the peak load. As expected, concrete specimens made without fibers (i.e., UHPC) showed a brittle failure, while concrete mixes made with fibers (i.e., UHPFRC) showed a ductile behavior and a greater load-carrying capacity and toughness. This can be attributed to the capability of fibers to bridge the micro and macro cracks.

Table 7 shows the flexural strength of all concrete mixes exposed to room temperature, 100°C, 300°C and 400°C. At room temperature, concrete specimens made without fibers (i.e., UHPC) showed a flexural strength of 10.3 MPa. In comparison, concrete specimens made with fibers showed a flexural strength that ranged from 16.9 MPa to 19.8 MPa, as shown in Table 7, which corresponds to an approximately 65% to 90% increase in the flexural strength. This can be attributed to the presence of fibers that increased the cracking resistance of the concrete. Concrete made with steel fibers showed the greatest increase in flexural strength

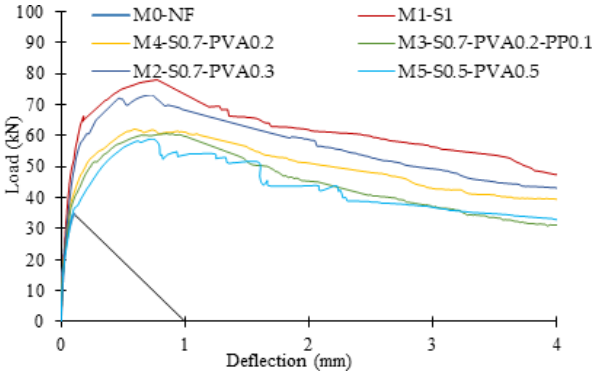

Fig. 11. Load-deflection relations for UHPC and UHPFRC beams (room temp. 26°C)

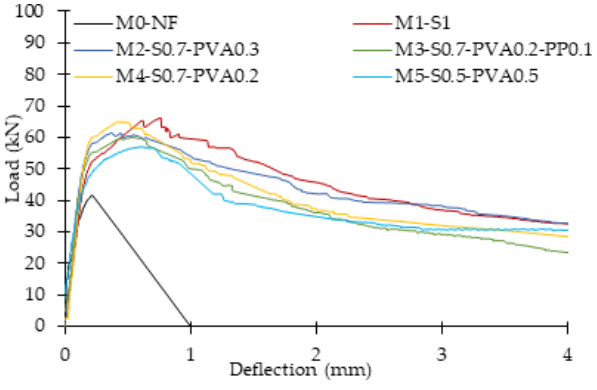

Fig. 12. Load-deflection relations for UHPC and UHPFRC beams (300°C)

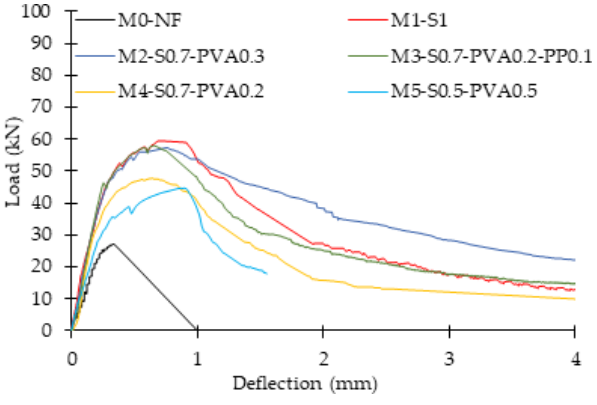

Fig. 13. Load-deflection relations for UHPC and UHPFRC beams (400°C)

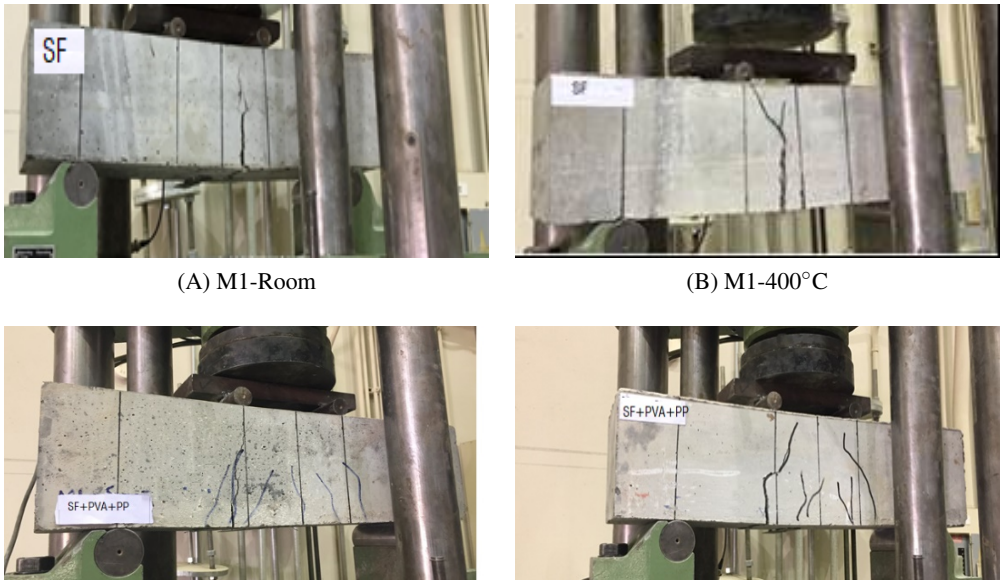

(A) M1-Room (B) M1-400°C

(C) M3-Room (D) M3-400°C

Fig. 14. Mode of failure of some representative concrete prisms

(i.e., 90%) compared to the control mix without fibers. The concrete mix made of 0.7% steel fibers and 0.3% PVA fibers showed an approximately 85% increase in flexural strength compared to the control mix without fibers. The remaining three concrete mixes made of a combination of either steel, PVA, and PP fibers or steel and PVA fibers showed approximately the same flexural strength at room temperature.

When the concrete was subjected to 100°C, the flexural strength was slightly increased by approximately 1% to 4% in all mixes. This can be due to the increased compressive strength that was previously reported when the concrete was exposed to temperatures of 100°C. After exposure to higher temperatures at 300°C and 400°C, concrete specimens made without fibers showed approximately 15% and 27% reduction in flexural strength, respectively, compared to the same concrete exposed to room temperature. The decrease in the flexural strength in concrete mixes made with fibers was approximately 4% to 9% after the exposure to 300°C and 11% to 25% when exposed to 400°C. Concrete mix made with a combination of steel, PP, and PVA fibers showed the lowest reduction in flexural strength when exposed to high temperature at 300°C and 400°C.

Concrete specimens made with fibers (i.e., UHPFRC) showed significantly greater ductility at failure and greater load-carrying capacity compared to concrete specimens without fibers (i.e., UHPC). The failure mode in concrete specimens without fibers was brittle, while a ductile failure with fewer and more distributed cracks was observed in concrete specimens made with fibers, as shown in Figure 14. Concrete specimens made with steel and PVA fibers showed extended softening behavior compared to concrete specimens made with steel fibers only. This indicates that using a hybrid system made with steel and PVA fibers was more efficient in increasing the cracking resistance of concrete compared to using steel fibers alone. In addition, the hybrid system made of steel and PVA fibers was more effective in controlling the cracking propagation compared to a hybrid system made with steel, PVA, and PP fibers. The results of this study are consistent with previous research on the effect of fibers on the flexural strength of concrete. For example, a study by Wu et al. [67] found that adding steel fibers to UHPC increased the flexural strength by up to 83%. Another study by Jiao et al. [70] found that the flexural strength of UHPC

decreased by up to 27% after exposure to 400°C. Overall, the study's findings suggest that adding fibers to UHPC can significantly increase its flexural strength and ductility, and using a hybrid system made with a combination of fibers can provide better cracking resistance and control of cracking propagation.

3.5. Splitting tensile strength

The results of the splitting tensile strength study are provided in Table 7. Concrete specimens exposed to room temperature showed a splitting tensile strength between 6.6 MPa and 12.3 MPa. Concrete specimens without fibers showed the lowest splitting tensile strength of 6.6 MPA. Concrete specimens made with fibers showed significantly greater splitting tensile strength between 11.3 MPa and 12.3 MPa, representing a 74% to 86% improvement. This is expected as the presence of fibers improved the cracking resistance of the concrete resulting in a higher splitting tensile strength. Concrete specimens without fibers revealed a brittle failure, while concrete made with fibers showed a ductile failure.

As observed previously with the compressive and flexural strength testing results, the exposure to an elevated temperature at 100°C caused an approximately 3% increase in the splitting tensile strength. This was attributed to the increase in the compressive strength due to the additional hydration reactions that occurred, causing increased strength. Furthermore, the elevated temperature exposure may also influence the pore structure and microstructure of the concrete. The heat can lead to the expansion of moisture within the concrete, creating internal pressure that further contributes to the densification of the material. This densification reduces the occurrence of voids and pore connectivity, which positively affects the strength of the concrete [59, 71]. When the concrete was exposed to high temperatures of 300°C and 400°C, the control mix made without fibers showed approximately 14% and 27% decrease in the splitting tensile strength compared to the same concrete mix exposed to room temperature. Alternatively, concrete mixes made with fibers showed lower reductions in the splitting tensile strength when subjected to temperatures at 300°C and 400°C. After exposure to 300°C, the reduction in the splitting tensile strength was 8% in the concrete mix made with steel fibers and 3% to 7% in concrete mixes made with steel and PVA fibers compared to those exposed only to room temperature. Concrete mix made with hybrid fibers consisting of steel, PVA, and PP fibers showed a 6% reduction when the concrete was exposed to 300°C. After exposure to 400°C, the reduction in the splitting tensile strength was 13% in the concrete mix made with steel fibers only, 13% to 22% in concrete mixes made of a combination of steel and PVA fibers, and 14% in concrete made with a hybrid of steel, PVA, and PP fibers compared to concrete exposed to room temperature. The experimental results of these findings match previous studies exploring the effects of fiber reinforcement and high temperatures on concrete properties. Doo et al. [72] and Doo and Shin [73] found that fibers enhance splitting tensile strength and crack resistance, consistent with current findings. Similarly, Chen et al. [45] showed that high temperatures decrease splitting tensile strength more in concrete without fiber reinforcement, in line with the experimental results.

3.6. Effect of fiber type

To evaluate the effect of fiber content and type on the mechanical characteristics of UHPC, the compressive, flexural, and splitting tensile strength results were normalized (i.e., the results at high temperature were divided by the results obtained at room temperature). The impact of high temperatures exposure on the normalized compressive, flexure, and splitting tensile strengths are presented in Figures 15 to 17, respectively.

In Figure 15, it can be observed that the addition of fibers caused a significant enhancement in the residual compressive strength after the exposure to high temperatures of 300°C and 400°C. It can also be observed from this figure that steel fibers were the most efficient in maintaining the compressive strength after the exposure to 300°C compared to the other hybrid fiber system. At 400°C, however,

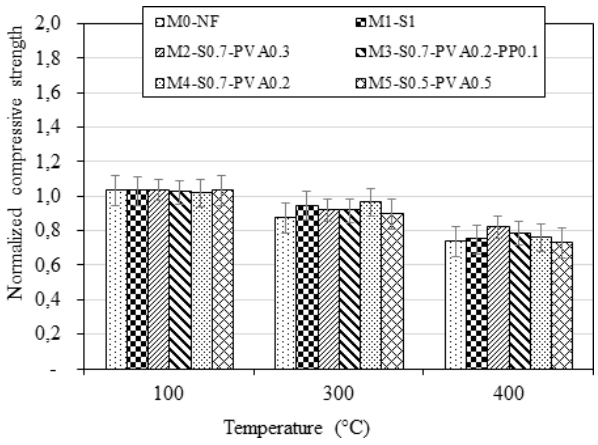

Fig. 15. Temperature effects on UHPC and UHPFRC normalized compressive strength

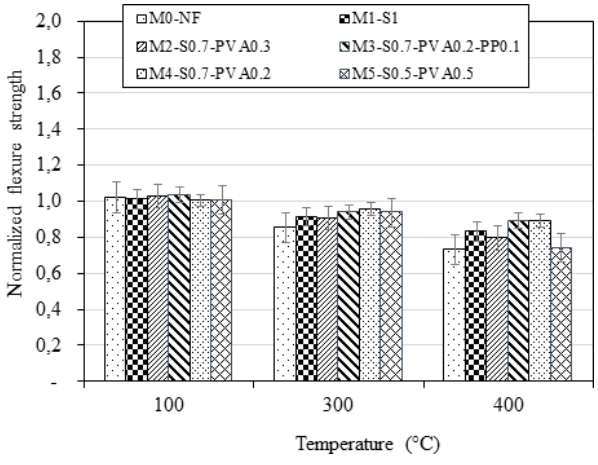

Fig. 16. Temperature effects on the normalized flexural strength of UHPC and UHPFRC

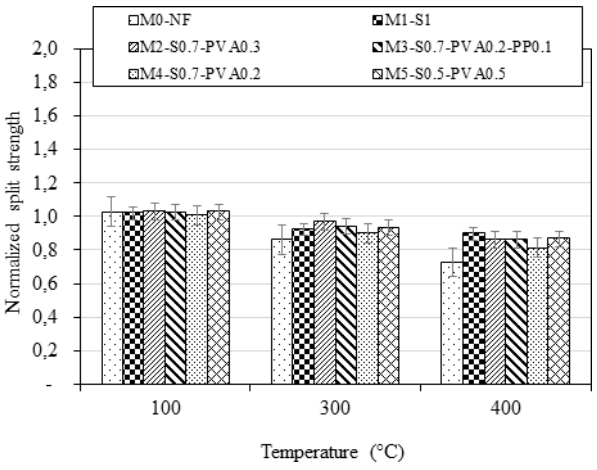

Fig. 17. Temperature effects on the normalized splitting tensile strength of UHPC and UHPFRC

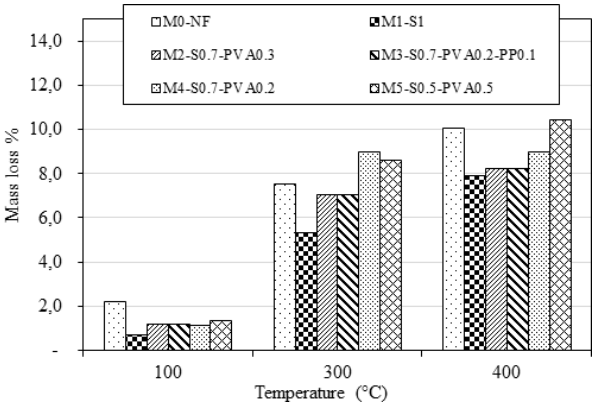

Fig. 18. Effect of temperature on weight loss for UHPC and UHFRC specimens

the hybrid fiber system, which included steel, PP, and PVA fibers, proved to be the most effective in maintaining the compressive strength compared to concrete specimens with steel fibers alone or a combination of steel and PVA fibers.

In Figure 16, it can be observed that hybrid systems consisting of steel and PVA fibers and steel, PVA and PP fibers were more effective in maintaining flexural strength after exposure to 300°C. Hybrid fiber consisting of steel, PP, and PVA fibers (i.e., mix M3-S0.7–PVA0.2–PP0.1) and mix M4-S0.7–PVA0.2 were the most efficient in maintaining the flexural strength after exposure to 400°C followed by steel fibers alone (M1-S1).

For the splitting tensile strength study, a combination of 0.7% steel fibers and 0.3% PVA fibers was the most effective in maintaining the splitting tensile strength after exposure to 300°C. All the fiber systems evaluated in this study showed approximately similar effectiveness in retaining the splitting tensile strength after exposure to 400°C.

In Figures 18 to 20, it can be observed that using steel fibers alone was the most effective in maintaining the mechanical characterization of UHPC exposed to high temperatures at 300°C and 400°C. Hybrid fibers made of steel, PP, and PVA fibers were the second most effective system, followed by a combination made of steel and PVA. Because of the melting and evaporation of PP fibers at high

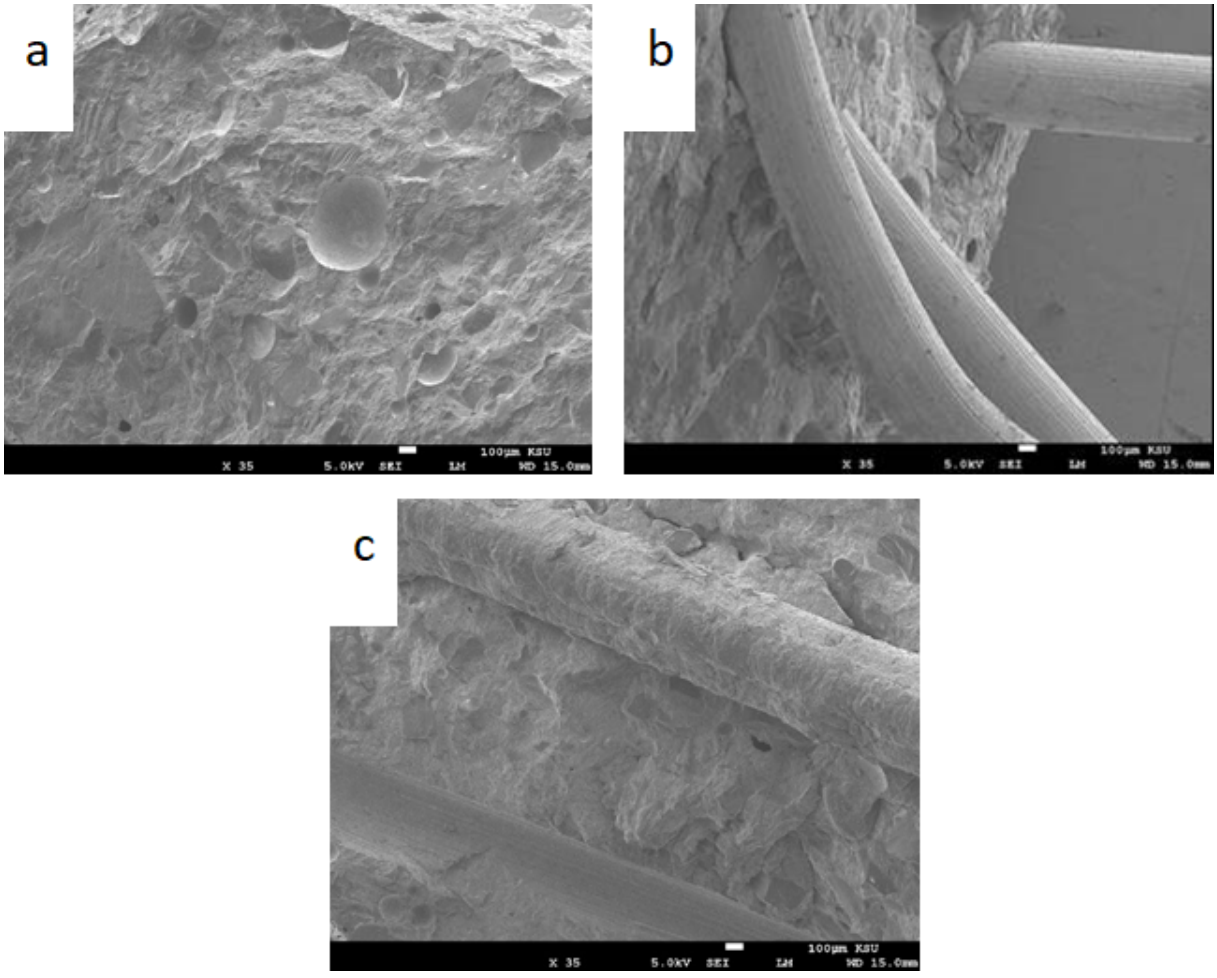

Fig. 19. Secondary electron SEM images of concrete exposed to room temperature (a) mix M0-NF, (b) M1-S1, and (c) M3-S0.5+PVA0.5

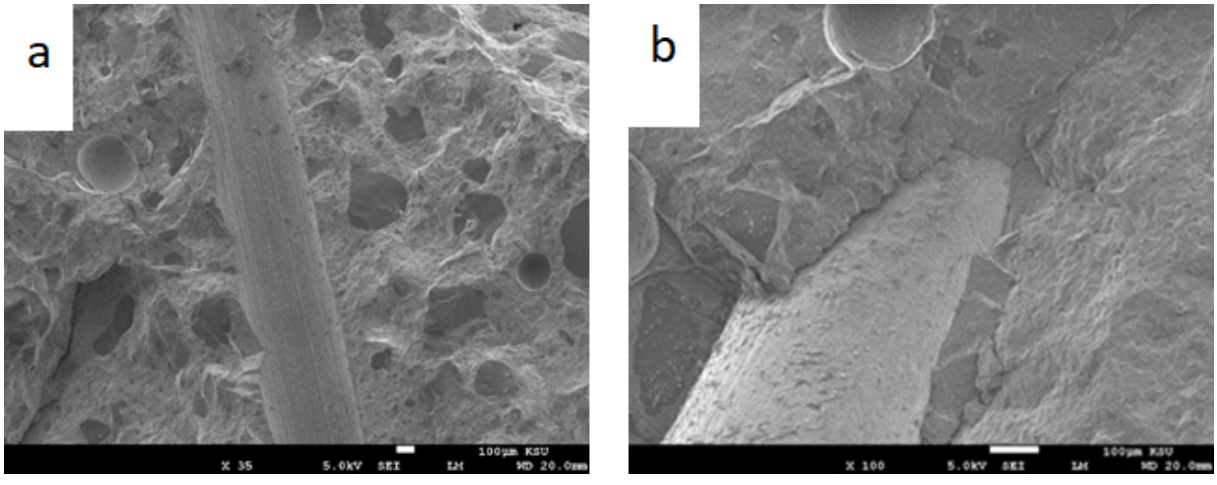

Fig. 20. Secondary electron SEM images of concrete containing steel fibers (i.e., M1-S1) after exposure to 400°C

temperatures, the inclusion of PP fibers improves the mechanical characteristics of UHPC by providing venting channels for lowering the vapor pressure inside the samples. The test results of UHPC made with hybrid fibers under elevated temperatures in this study are consistent with findings in the literature. The addition of fibers, particularly steel fibers, significantly enhanced the residual compressive strength after exposure to high temperatures of 300°C and 400°C, which is in line with the results reported in previous studies [74–76].

3.7. Mass loss

A mass reduction is expected when concrete is subjected to elevated temperatures due to free and chemical water loss. The initial mass was measured before placing the test specimen in the furnace. The final mass of the samples was considered to be the mass after reaching target temperature. To calculate the percentage of mass loss of the UHPC and UHPFRC specimens due to elevated temperatures, the weights of the specimens were recorded before and after exposure to the elevated temperature. Because of rapid drying, the weight loss from UHPC increases as the severe temperature increases. The variation in mass loss and temperature is depicted in Figure 18. All samples were heated to the target temperature with an exposure duration of 3 hours. The findings indicated that the mass loss increases with increasing temperature and the extreme increase at 400°C occurs within a 3-hour exposure time. It can be noted that the concrete specimens containing a higher content of steel fiber show less mass loss at higher temperature exposure than specimens with a higher content of synthetic fibers, as a result of the melting of polypropylene and polyvinyl alcohol fiber. Several studies have investigated the mass loss of UHPC made with different types of fibers when exposed to elevated temperatures. A study by Li et al. [74] investigated the effect of different types of fibers, including steel fibers, polypropylene fibers, and hybrid fibers, on the mass loss of UHPC exposed to high temperatures of up to 1000°C. The study found that UHPC with steel fibers exhibited the highest mass loss, followed by UHPC with polypropylene fibers and hybrid fibers. The addition of hybrid fibers reduced the mass loss of UHPC compared to UHPC with only steel or polypropylene fibers. The study also found that the addition of hybrid fibers improved the residual compressive strength and ductility of UHPC after exposure to high temperatures. A study by Chen et al. [45] investigated the effect of hybrid fiber on the mass loss of UHPC exposed to high temperatures up to 1200°C. The study found that UHPC with hybrid fibers exhibited lower mass loss than UHPC without fibers or with only steel fibers. The study also found that the addition of hybrid fibers improved the thermal stability of UHPC and reduced the rate of strength loss at elevated temperatures. Another finding by Yang et al. [76] investigated the effect of hybrid fiber on the mass loss of UHPC exposed to high temperatures up to 1000°C. The study found that UHPC with hybrid fibers exhibited lower mass loss than UHPC without fibers or with only steel fibers. The study also found that the addition of hybrid fibers improved the spalling resistance of UHPC and reduced the severity of spalling.

3.8. Microstructural analysis using SEM

In addition to the mechanical properties evaluated in this study, microstructure analysis using scanning electron microscopy on fracture surfaces was used to evaluate the microstructure of each mix before and after exposure to high temperature at 400°C. One sample was extracted from each of the six mixes before and after exposure to 400°C. Once the sample was removed from the cylinder, it was stored in a sealed container containing soda-lime and silica gel to prevent any carbonation or further hydration. At the testing time, a fresh-fracture surface was exposed from each sample before SEM testing. Figure 19 presents secondary electron images of concrete mixes before exposure to high temperature. Figures 20 and 21 present secondary electron images of concrete mixes after exposure to high temperature at 400°C.

In Figure 19, it can be observed that the microstructure is dense as a result of the lower water-to-cement ratio and the use of micro silica, causing additional hydration products that densify the

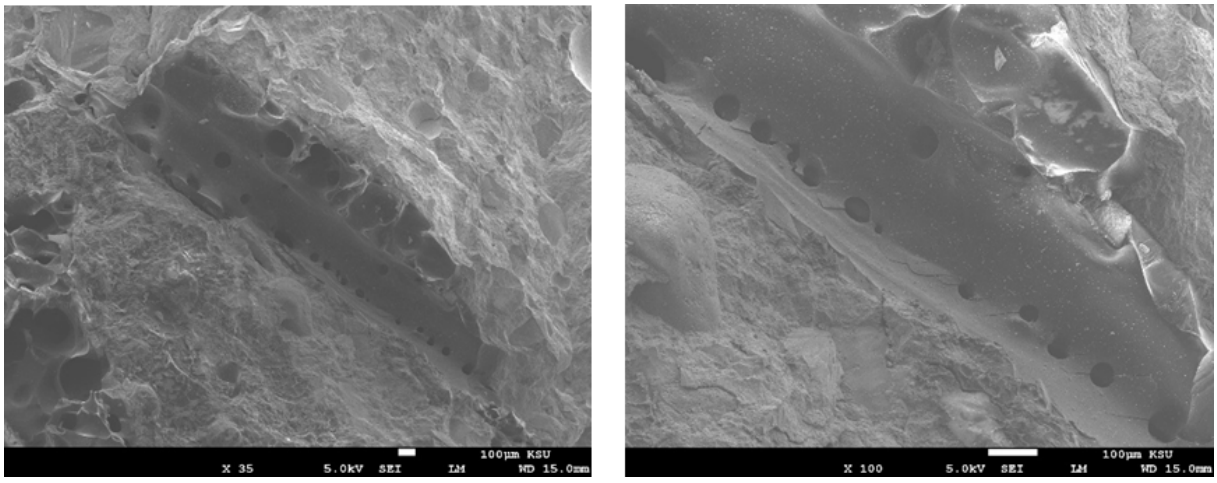

Fig. 21. Secondary electron SEM images of concrete containing PVA fibers (i.e., M3-S0.7-PVA0.2-PP0.1) after exposure to 400°C

microstructure. The microstructural analysis also showed well distributed fine aggregates with no entrapped air voids. The exposure to high temperature at 400°C caused degradation at the interface between the hydrated cement matrix and the steel fibers. The decomposition of the cement matrix caused this degradation at the interface and the yielding of steel fibers. The decomposition of the cement matrix includes the complete decomposition of ettringite and the loss of chemically bonded water. Figure 20b shows a gap between the hydrated cement matrix and the steel fibers caused by this degradation. Concrete made with PVA fibers showed empty spaces occupied by the PVA fibers before melting and evaporating, as shown in Figure 21. The shape confirmed this and the size of the empty voids, because the PVA fibers had a circular cross-section of 0.06 mm. The network of voids that were previously occupied by PVA fibers aided in releasing the vapor pressure build-up due to the exposure to 400°C temperatures [77]. Studies by Zhang et al. [78] and Li et al. [74] revealed that thermal decomposition of ettringite and C-S-H gel breakdown cause significant microstructural changes in UHPC. UHPC with PVA or polypropylene fibers showed more damage, while UHPC with steel fibers caused fiber/matrix interface debonding and cracking. The fiber type and exposure temperature determine fiber effects.

4. Conclusions

On the basis of the findings of this research, the following outcomes can be drawn:

1. The use of steel fibers or a hybrid of steel, PP and PVA fibers increases the compressive strength of concrete by approximately 6% to 17% when the concrete is exposed to room temperature at 27°C.
2. The mechanical properties including compressive, flexure, and splitting tensile strengths of concrete, were slightly improved by approximately 1% to 4% when the concrete was exposed to 100°C. This improvement was attributed to the additional hydration reactions that improved the microstructure of the concrete.
3. UHPFRC made of steel fibers can maintain a significant portion of its mechanical properties after exposure to high temperature at 300°C. No spalling was observed at 300°C. After exposure to 400°C, however, spalling occurred in the concrete and at 500°C, the concrete was completely damaged.
4. UHPFRC made with steel fibers alone or made with hybrid fibers showed a ductile behavior when tested for compression, flexure, or splitting tensile strength. This ductility behavior of concrete was not impacted when

the concrete was exposed to high temperatures. On the other hand, UHPFRC made with a combination of steel, PP, and PVA fibers showed ductile behavior at ambient temperature and a brittle response when subjected to high temperatures at 300°C and 400°C.

5. The compressive, flexural, and splitting strength decreased with the increase in the exposure temperature. This decrease was less pronounced in concrete mixes made with higher fiber content. This indicates that increasing fiber content can improve the concrete resistance to high temperatures.
6. Steel fibers alone were the most effective fiber system to maintain the mechanical properties of UHPFRC exposed to high temperatures at 300°C and 400°C followed by a hybrid fiber system made of steel, PP, and PVA fibers and a hybrid system made of steel and PVA fibers.
7. The use of PP fibers and PVA improved the mechanical properties of concrete due to the melting and evaporation of these fibers at severe temperatures, generating venting cannels that minimize the inner vapor pressure, which was confirmed using scanning electron microscopy.
8. The microstructure analyzed showed that the UHPC without fibers produced enormous cracks, while the UHPC with hybrid fibers did not develop cracks; instead, these pores, which were created by the fusing of the fibers, allowed substantial amounts of heat to escape. The UHPC without fibers as a result showed more damage than the UHPC with fibers.

Conflict of interest

None

Acknowledgements

The authors extend their appreciation to Researchers Supporting Project number (RSP2023R343), King Saud University, Riyadh, Saudi Arabia.

References

[1] Ding M, Yu R, Feng Y, Wang S, Zhou F, Shui Z, Gao X, He Y, Chen L. Possibility and advantages of producing an ultra-high performance concrete (UHPC) with ultra-low cement content. *Constr Build. Mater.* 2021; 273:122023. https://doi.org/10.1016/j.conbuildmat.2020.122023.

[2] Yu R, Spiesz P, Brouwers HJH. Development of an eco-friendly ultra-high performance concrete (UHPC) with efficient cement and mineral admixtures uses. 2014.

[3] Li Y, Tan KH, Yang EH. Influence of aggregate size and inclusion of polypropylene and steel fibers on the hot permeability of ultra-high performance concrete (UHPC) at elevated temperature. *Constr Build Mater.* 2018; 169:629–637. https://doi.org/10.1016/j.conbuildmat.2018.01.105.

[4] Arora A, Yao Y, Mobasher B, Neithalath N. Fundamental insights into the compressive and flexural response of binder- and aggregate-optimized ultra-high performance concrete (UHPC). *Cem Concr Compos.* 2019; 98:1–13. https://doi.org/10.1016/j.cemconcomp.2019.01.015.

[5] Hassan M, Wille K. Experimental impact analysis on ultra-high performance concrete (UHPC) for achieving stress equilibrium (SE) and constant strain rate (CSR) in Split Hopkinson pressure bar (SHPB) using pulse shaping technique. *Constr Build Mater.* 2017; 144:747–757. https://doi.org/10.1016/j.conbuildmat.2017.03.185.

[6] Yang J, Chen B, Su J, Xu G, Zhang D, Zhou J. Effects of fibers on the mechanical properties of UHPC: a review. *J Traffic Transp Eng*. 2022; 9:363–387. https://doi.org/10.1016/j.jtte.2022.05.001.

[7] Meng W, Khayat K. Effect of hybrid fibers on fresh, mechanical properties, and autogenous shrinkage of cost effective UHPC. *J Mater Civ Eng*. 2018; 30. https://doi.org/10.1061/(ASCE)MT.1943-5533.0002212.

[8] Xu L, Lu Q, Chi Y, Yang Y, Yu M, Y. Yan Y. Axial compressive performance of UHPC filled steel tube stub columns containing steel-polypropylene hybrid fiber. *Constr Build Mater*. 2019; 204:754–767. https://doi.org/10.1016/j.conbuildmat.2019.01.202.

[9] Su Y, Li J, Wu C, Wu P, Li Z.-X. Effects of steel fibres on dynamic strength of UHPC. *Constr Build Mater.* 2016; 114:708–718. https://doi.org/10.1016/j.conbuildmat.2016.04.007.

[10] Zeng X, Deng K, Liang H, Xu R, Zhao C, Cui B. Uniaxial behavior and constitutive model of reinforcement confined coarse aggregate UHPC. *Eng Struct.* 2020; 207:110261. https://doi.org/10.1016/j.engstruct.2020.110261.

[11] Zhang Y, Li X, Zhu Y, Shao X. Experimental study on flexural behavior of damaged reinforced concrete (RC) beam strengthened by toughness-improved ultra-high performance concrete (UHPC) layer. Compos Part B Eng. 2020; 186:107834. https://doi.org/10.1016/j.compositesb.2020.107834.

[12] Ghafari E, Costa H, Júlio E. RSM-based model to predict the performance of self-compacting UHPC reinforced with hybrid steel micro-fibers. *Constr Build Mater.* 2014; 66:375–383. https://doi.org/10.1016/j.conbuildmat.2014.05.064.

[13] Thomas RJ, Sorensen AD. Review of strain rate effects for UHPC in tension. *Constr Build Mater*. 2017; 153:846–856. https://doi.org/10.1016/j.conbuildmat.2017.07.168.

[14] Ozawa M, Subedi Parajuli S, Uchida Y, Zhou B. Preventive effects of polypropylene and jute fibers on spalling of UHPC at high temperatures in combination with waste porous ceramic fine aggregate as an internal curing material. *Constr Build Mater*. 2019; 206:219–225. https://doi.org/10.1016/j.conbuildmat.2019.02.056.

[15] Yu R, Spiesz P, Brouwers HJH. Effect of nano-silica on the hydration and microstructure development of ultra-high performance concrete (UHPC) with a low binder amount. *Constr Build Mater.* 2014; 65:140–150. https://doi.org/10.1016/j.conbuildmat.2014.04.063.

[16] Qian D, Yu R, Shui Z, Sun Y, Jiang C, Zhou F, Ding M, Tong X, He Y. A novel development of green ultra-high performance concrete (UHPC) based on appropriate application of recycled cementitious material. *J Clean Prod.* 2020; 261:121231. https://doi.org/10.1016/J.JCLEPRO.2020.121231.

[17] Kheir J, Klausen A, Hammer TA, De Meyst L, Hilloulin B, Van Tittelboom K, Loukili A, De Belie N. Early age autogenous shrinkage cracking risk of an ultra-high performance concrete (UHPC) wall: modelling and experimental results. *Eng Fract Mech*. 2021; 257:108024. https://doi.org/10.1016/j.engfracmech.2021.108024.

[18] Li S, Tang L, Shi W, Zhong C. Experimental investigation on hydroabrasive erosion of steel fiber UHPC and rubber UHPC. *Adv Mater Sci Eng*. 2020; 2020:5920824. https://doi.org/10.1155/2020/5920824.

[19] Jia L, Fang Z, Huang Z, Pilakoutas K, Wang Q, Tan X. Flexural behavior of UHPC beams prestressed with external CFRP tendons. *Appl Sci*. 2021; 11:9189. https://doi.org/10.3390/app11199189.

[20] Kalifa P, Chéné G, Gallé C. High-temperature behaviour of HPC with polypropylene fibres—from spalling to microstructure. *Cem Concr Res*. 2001; 31:1487–1499. https://doi.org/10.1016/S0008-8846(01)00596-8.

[21] Noumowé A, Carré H, Daoud A, Toutanji H. High-strength self-compacting concrete exposed to fire test. *J Mater Civ Eng.* 2006; 18:754–758. https://doi.org/10.1061/(asce)0899-1561(2006)18:6(754).

[22] PhanL.Spalling and mechanical properties of high strength concrete at high temperature. *Proc Concr under Sev Cond Fr*. 2007; 1595–1608. http://fire.nist.gov/bfrlpubs/build07/art019.html (accessed December 26, 2021).

[23] Chan SYN, X. Luo X, Sun W. Efect of high temperature and cooling regimes on the compressive strength and pore properties of high performance concrete. *Constr Build Mater.* 2000; 14:261–266. https://doi.org/10.1016/S0950-0618(00)00031-3.

[24] Aslani F, Bastami M Constitutive relationships for normal-and high-strength concrete at elevated temperatures. *ACI Mater J*. 2011; 108:355–364. https://doi.org/10.14359/51683106.

[25] Lau A, Anson M. Effect of high temperatures on high performance steel fibre reinforced concrete. *Cem Concr. Res*. 2006; 36:1698–1707. https://doi.org/10.1016/j.cemconres.2006.03.024.

[26] Varona FB, Baeza FJ, Bru D, Ivorra S. Influence of high temperature on the mechanical properties of hybrid fibre reinforced normal and high strength concrete, *Constr Build Mater*. 2018; 159:73–82. https://doi.org/10.1016/J.CONBUILDMAT.2017.10.129.

[27] Mindess S, Young JF, Darwin DC. 2nd ed.; Upper Saddle River, NJ: Prentice-Hall; 2003.

[28] Liu CT, Huang JS. Fire performance of highly flowable reactive powder concrete. *Constr Build Mater*. 23 (2009) 2072–2079. https://doi.org/10.1016/j.conbuildmat.2008.08.022.

[29] Bazant ZP, Thonguthai W. Pore pressure and drying of concrete at high temperature. *ASCE J Eng Mech Div*. 1978; 104:1059–1079. https://doi.org/10.1061/jmcea3.0002404.

[30] Zohrevand P, Mirmiran P. Behavior of ultrahigh-performance concrete confined by fiber-reinforced polymers. *J Mater Civ Eng*. 2011; 23:1727–1734. https://doi.org/10.1061/(ASCE)MT.1943-5533.0000324.

[31] Mróz K, Hager I. Evaluation of nature and intensity of fire concrete spalling by frequency analysis of sound records. *Cem Concr. Res*. 2021; 148:106539. https://doi.org/10.1016/J.CEMCONRES.2021.106539.

[32] Abadel A, Elsanadedy H, Almusallam T, Alaskar A, Abbas H, Al-Salloum Y. Residual compressive strength of plain and fiber reinforced concrete after exposure to different heating and cooling regimes. 2021; 26:6746–6765. https://doi.org/10.1080/19648189.2021.1960898.

[33] Zhang D, Tan KH. Effect of various polymer fibers on spalling mitigation of ultra-high performance concrete at high temperature. *Cem Concr Compos*. 2020; 114: 103815. https://doi.org/10.1016/j.cemconcomp.2020.103815.

[34] Travis QB, Mobasher B. Correlation of elastic modulus and permeability in concrete subjected to elevated temperatures. *J Mater Civ Eng*. 2010; 22:735–740. https://doi.org/10.1061/(asce)mt.1943-5533.0000074.

[35] Gallé C, Sercombe J. Permeability and pore structure evolution of silico-calcareous and hematite high-strength concretes submitted to high temperatures. *Mater Struct Constr*. 2001; 34:619–628. https://doi.org/10.1617/13695.

[36] Wille K, Naaman AE, Parra-Montesinos GJ. Ultra-high performance concrete with compressive strength exceeding 150 MPa (22 ksi): a simpler way. *ACI Mater J*. 2011; 108:46–54. https://doi.org/10.14359/51664215.

[37] Richard P, Cheyrezy M. Composition of reactive powder concretes. *Cem Concr Res*. 1995; 25:1501–1511. https://doi.org/10.1016/0008-8846(95)00144-2.

[38] Klingsch EW, Frangi A, Fontana M. High- and ultrahigh-performance concrete: a systematic experimental analysis on spalling. *Am Concr Institute, ACI Spec. Publ*. 2011; 279:269–318.

[39] Diederichs U, Mertzsch O. Behaviour of ultra high strength concrete at high temperatures. In: Kassel, Ed. Second International Symposium on Ultra High Performance Concrete. 2008, pp. 347–354.

[40] Peng GF, Kang YR, Huang YZ, Liu XP, Chen Q. Experimental research on fire resistance of reactive powder concrete. *Adv Mater Sci Eng*. 2012. https://doi.org/10.1155/2012/860303.

[41] Varona FB, Baeza FJ, Bru D, Ivorra S. Influence of high temperature on the mechanical properties of hybrid fibre reinforced normal and high strength concrete, *Constr Build Mater*. 2018; 159:73–82. https://doi.org/10.1016/j.conbuildmat.2017.10.129.

[42] Bangi MR, Horiguchi T. Effect of fibre type and geometry on maximum pore pressures in fibre-reinforced high strength concrete at elevated temperatures. *Cem Concr Res*. 2012; 42:459–466. https://doi.org/10.1016/J.CEMCONRES.2011.11.014.

[43] Novák J, Kohoutková A. Fire response of hybrid fiber reinforced concrete to high temperature. *Procedia Eng*. 2017; 172:784–790. https://doi.org/10.1016/J.PROENG.2017.02.123.

[44] Heinz D, Ludwig H-M. Heat treatment and the risk of DEF delayed ettringite formation in UHPC. In: International Symposium on Ultra High Performance Concrete in Kassel, Germany. 2004; pp. 717–730.

[45] Chen HJ, Yu YL, Tang CW. Mechanical properties of ultra-high performance concrete before and after exposure to high temperatures. *Materials* (Basel). 2020; 13:770. https://doi.org/10.3390/ma13030770.

[46] Tayeh B, Hadzima-nyarko M, Youssef M, Riad R, Defalla R, Hafez A. Behavior of ultra-high-performance concrete with hybrid synthetic fiber waste exposed to elevated temperatures. 2023; 13:129.

[47] ISO, Elements of building construction - Part 1: General requirements. International Organization for Standardization, Geneva, Switzerland. 1999.

[48] ASTM international, standard test method for slump of hydraulic-cement concrete. ASTM C143-10a. 2010; 13:1–4.

[49] ASTM C138/C138M-17a, No title standard test method for density (unit weight), yield, and air content (gravimetric) of concrete. ASTM Int. 2017. https://doi.org/10.1520/C0138_C0138M-17A.

[50] ASTM-C39, standard test method for compressive strength of cylindrical concrete. *Annu B ASTM Stand*. 2021; 10:1520. https://doi.org/D.0.I:10.1520/C0039_C0039M-10.

[51] ASTM C469-02, standard test method for static modulus of elasticity and poisson's ratio of concrete in compression. *ASTM Stand. B*. 2002; 04:1–5. http://portales.puj.edu.co/wjfajardo/mecanicadesolidos/laboratorios/astm/C469.pdf.

[52] ASTM C496-96, standard test method for splitting tensile strength of cylindrical concrete specimens. *Man Hydrocarb Anal 6th Ed*. 2008; i:545-545–3.

[53] A. C78/C78M-16, standard test method for flexural strength of concrete (using simple beam with third-point loading). *ASTM Int*. 2016. https://doi.org/10.1520/C0078_C0078M-16.

[54] Bisby LA, Chen JF, Li SQ, Stratford TJ, Cueva , Crossling K. Strengthening fire-damaged concrete by confinement with fibre-reinforced polymer wraps. *Eng Struct*. 2011; 33:3381–3391. https://doi.org/10.1016/J.ENGSTRUCT.2011.07.002.

[55] Abadel AA, Alharbi YR. Confinement effectiveness of CFRP strengthened ultra-high performance concrete cylinders exposed to elevated temperatures. *Mater Sci*. 2021; 39:478–490. https://doi.org/10.2478/MSP-2021-0040.

[56] Ju Y, Wang L, Liu H, Tian K. An experimental investigation of the thermal spalling of polypropylene-fibered reactive powder concrete exposed to elevated temperatures. *Sci Bull*. 2015; 60:2022–2040. https://doi.org/10.1007/S11434-015-0939-0.

[57] Novák J, Kohoutková A. Fibre reinforced concrete exposed to elevated temperature. IOP Conference Series Materials Science and Engineering. 2017; 246:012045. https://doi.org/10.1088/1757-899X/246/1/012045.

[58] Bangi MR, Horiguchi T. Effect of fibre type and geometry on maximum pore pressures in fibre-reinforced high strength concrete at elevated temperatures. *Cem Concr Res*. 2012; 42:459–466. https://doi.org/10.1016/j.cemconres.2011.11.014.

[59] Hager I, Zdeb T, Krzemié K. The impact of the amount of polypropylene fibres on spalling behaviour and residual mechanical properties of reactive powder concretes. *MATEC Web Conference*. 2013; 6:2003. https://doi.org/10.1051/matecconf/20130602003.

[60] Peng GF, Chan SYN, Anson M. Chemical kinetics of C-S-H decomposition in hardened cement paste subjected to elevated temperatures up to 800°C. 2015; 13:47–52. https://doi.org/10.1680/ADCR.2001.13.2.47.

[61] Scheinherrová L, Vejmelková E, Keppert M, Bezdička P, Doleželová M, Krejsová J, Grzeszczyk S, Matuszek-Chmurowska A, Černý R. Effect of Cu-Zn coated steel fibers on high temperature resistance of reactive powder concrete. *Cem Concr Res*. 2019; 117:45–57. https://doi.org/10.1016/J.CEMCONRES.2018.12.008.

[62] Ramezani M, Dehghani A, Sherif MM. Carbon nanotube reinforced cementitious composites: a comprehensive review. *Constr Build Mater*. 2022; 315:125100. https://doi.org/10.1016/J.CONBUILDMAT.2021.125100.

[63] Abadel AA, Abbas H., Alshaikh IMH, Sennah K, Tuladhar R, Altheeb A, Alamri M. Experimental study on the effects of external strengthening and elevated temperature on the shear behavior of ultra-high-performance fiber-reinforced concrete deep beams. *Structures*. 2023; 49:943–957. https://doi.org/10.1016/j.istruc.2023.02.004.

[64] Ambily PS, Ravisankar K, Umarani C, Dattatreya JK. Iyer NR. Development of ultra-high-performance geopolymer concrete. *Concr Res*. 2014; 66:82–89. https://doi.org/10.1680/macr.13.00057.

[65] Peng NR, Bian SH, Guo ZQ, Zhao J, Peng XL, Jiang YC. Effect of thermal shock due to rapid cooling on residual mechanical properties of fiber concrete exposed to high temperatures. *Constr Build Mater*. 2008; 22:948–955. https://doi.org/10.1016/j.conbuildmat.2006.12.002.

[66] Zhang P, Zhang P, Wu J, Zhang Y, Guo J. Mechanical properties of polyvinyl alcohol fiber-reinforced cementitious composites after high-temperature exposure. *Gels*. 2022; 8:662. https://doi.org/10.3390/GELS8100662.

[67] Wu Z, Shi C, He W, Wu L. Effects of steel fiber content and shape on mechanical properties of ultra high performance concrete. *Constr Build Mater*. 2016; 103:8–14. https://doi.org/10.1016/J.CONBUILDMAT.2015.11.028.

[68] Tahwia AM, Elgendy GM, Amin M. Durability and microstructure of eco-efficient ultra-high-performance concrete. *Constr Build Mater*. 2021; 303:124491. https://doi.org/10.1016/j.conbuildmat.2021.124491.

[69] Gong J, Ma Y, Fu J, Hu J, Ouyang X, Zhang Z, Wang H. Utilization of fibers in ultra-high performance concrete: a review. *Compos Part B Eng*. 2022; 241:109995. https://doi.org/10.1016/j.compositesb.2022.109995.

[70] Jiao C, Ta J, Niu Y, Meng S, Chen XF, He S, Ma R. Analysis of the flexural properties of ultra-high-performance concrete consisting of hybrid straight steel fibers. *Case Stud Constr Mater*. 2022; 17:e01153. https://doi.org/10.1016/J.CSCM.2022.E01153.

[71] Abid M, Hou X, Zheng W, Hussain RR. High temperature and residual properties of reactive powder concrete – a review. *Constr Build Mater*. 2017; 147:339–351. https://doi.org/10.1016/J.CONBUILDMAT.2017.04.083.

[72] Yoo D-Y, Banthia N, Lee J-Y, Yoon Y-S. Effect of fiber geometric property on rate dependent flexural behavior of ultra-high-performance cementitious composite. *Cem Concr Compos*. 2018; 86:57–71. https://doi.org/10.1016/j.cemconcomp.2017.11.002.

[73] Yoo DY, Shin W. Improvement of fiber corrosion resistance of ultra-high-performance concrete by means of crack width control and repair. *Cem Concr Compos*. 2021; 121:104073. https://doi.org/10.1016/J.CEMCONCOMP.2021.104073.

[74] Li Y, Tan KH, Yang EH. Synergistic effects of hybrid polypropylene and steel fibers on explosive spalling prevention of ultra-high performance concrete at elevated temperature. *Cem Concr Compos*. 2019; 96:174–181. https://doi.org/10.1016/J.CEMCONCOMP.2018.11.009.

[75] Ozawa M, Morimoto H. Effects of various fibres on high-temperature spalling in high-performance concrete. *Constr Build Mater*. 2014; 71:83–92. https://doi.org/10.1016/j.conbuildmat.2014.07.068.

[76] Xiao L, Chen P, Huang J, Peng S, Yang Z. Compressive behavior of reinforced steel-PVA hybrid fiber concrete short columns after high temperature exposure. *Constr Build Mater*. 2022; 342:127935. https://doi.org/10.1016/J.CONBUILDMAT.2022.127935.

[77] Xiao J, Falkner H. On residual strength of high-performance concrete with and without polypropylene fibres at elevated temperatures. *Fire Saf J*. 2006; 41:115–121. https://doi.org/10.1016/J.FIRESAF.2005.11.004.

[78] Zhang D, Tan KH, Dasari A, Weng Y. Effect of natural fibers on thermal spalling resistance of ultra-high performance concrete. *Cem Concr Compos*. 2020; 109:103512. https://doi.org/10.1016/j.cemconcomp.2020.103512.

Received 2023-03-27
Accepted 2023-06-07